Nanoscale Research Letters
a SpringerOpen Journal

NANO EXPRESS Open Access

Ethylenediaminetetraacetic acid as capping ligands for highly water-dispersible iron oxide particles

Yunfeng Yi[1,3†], Ying Zhang[2†], Yixiao Wang[3], Lihua Shen[3], Mengmeng Jia[3], Yu Huang[3], Zhenqing Hou[3*] and Guohong Zhuang[4,5*]

Abstract

Monodispersed magnetite (Fe_3O_4) particles were synthesized using a high-temperature hydrolysis reaction with the assistance of ethylenediaminetetraacetic acid (EDTA) as capping ligands. These particles were composed of small primary nanocrystals and their sizes could be tuned from about 400 to about 800 nm by simply changing the EDTA or precursor concentration. Surface-tethered EDTA made the particles highly water-dispersible. The as-prepared magnetite particles also showed superparamagnetic behavior at room temperature, and their magnetic properties were size dependent. In addition, the particles had a strong response to external magnetic field due to their high magnetization saturation values. These properties were very important for some potential biomedical applications, such as magnetic separation and magnetic-targeted substrate delivery.

Keywords: Magnetite; Magnetic properties; Nanocrystalline materials

Background

Over the past decade, magnetic nanocrystals (e.g., Fe_3O_4, γ-Fe_2O_3) have attracted much attention due to their unique magnetic properties and important applications such as targeted drug delivery [1,2], biomolecular separations [3,4], treatment of hyperthermia in cancer [5,6], and as contrast agents in magnetic resonance imaging (MRI) [7,8]. Up to now, many methods have been developed to prepare Fe_3O_4 nanocrystals with small sizes on the nanometer scale, which include hydrothermal synthesis [9,10], chemical coprecipitation [11-13], and thermal decomposition and/or reduction [14,15]. Besides these nanosized particles, the secondary structural superparamagnetic Fe_3O_4 particles have also attracted increasing attention due to their practical applications in magnetic separation and magnetic-targeted substrate delivery [16,17]. Generally, these secondary structural Fe_3O_4 particles consist of small Fe_3O_4 nanocrystals. As-prepared Fe_3O_4 particles are stable in solution and reveal rapid magnetic response to the externally applied magnetic field. Over the past decade, these secondary structural Fe_3O_4 particles are prepared by a common two-step process, including cooperative assembly [18], microemulsion templating [19], and spontaneous assembly [20]. Compared to the two-step process of assembling the pre-synthesized Fe_3O_4 nanocrystals into uniform secondary structures, the direct one-step growth route to synthesize the secondary structural Fe_3O_4 particles seems to be a simpler way, which is also economical for large-scale production.

Herein we reported a general approach for the fabrication of monodispersed, highly water-dispersible, and superparamagnetic Fe_3O_4 particles by a one-step hydrothermal procedure using an ethylenediaminetetraacetic acid (EDTA)-assisted route. Biocompatible EDTA was chosen because it can act as a crystal grain growth inhibitor for the synthesis of variously sized Fe_3O_4 particles, and the carboxylate groups of EDTA have a strong coordination affinity to the iron cations on the Fe_3O_4 surface, which might favor the attachment of hydrophilic groups on the surface of the Fe_3O_4 particles. Herein, the Fe_3O_4 particles synthesized with the assistance of EDTA were also intrinsically stabilized with a layer of hydrophilic

* Correspondence: houzhenqing@xmu.edu.cn; zhgh@xmu.edu.cn
†Equal contributors
[3]Research Center of Biomedical Engineering, Department of Biomaterials, College of Materials, Xiamen University, Xiamen 361005, China
[4]Organ Transplantation Institute, Medical College, Xiamen University, Xiamen 361005, China
Full list of author information is available at the end of the article

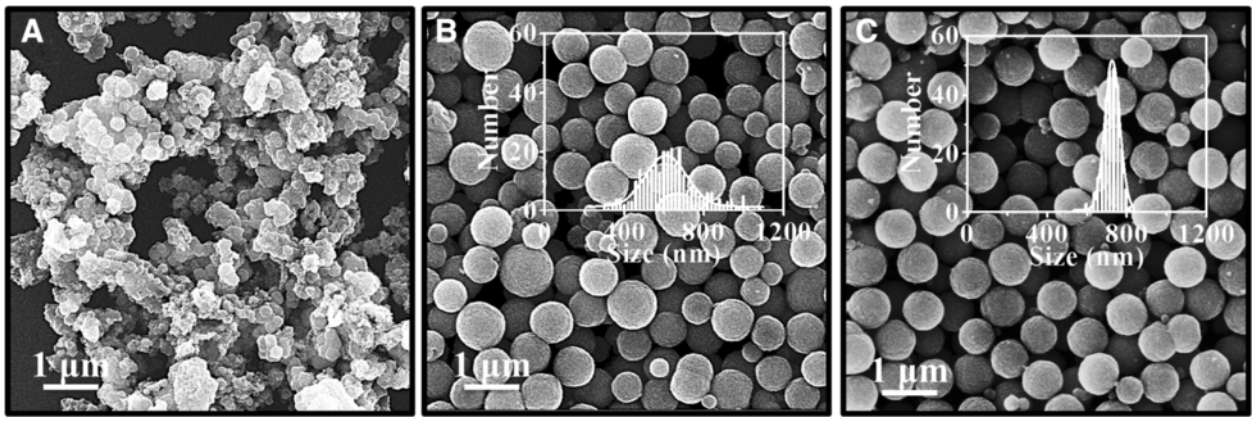

Figure 1 TEM images of Fe_3O_4 particles synthesized with different $FeCl_3$ concentrations. (A) 0.05. **(B)** 0.10. **(C)** 0.20 mol L^{-1}. Inset is the corresponding particle size distribution.

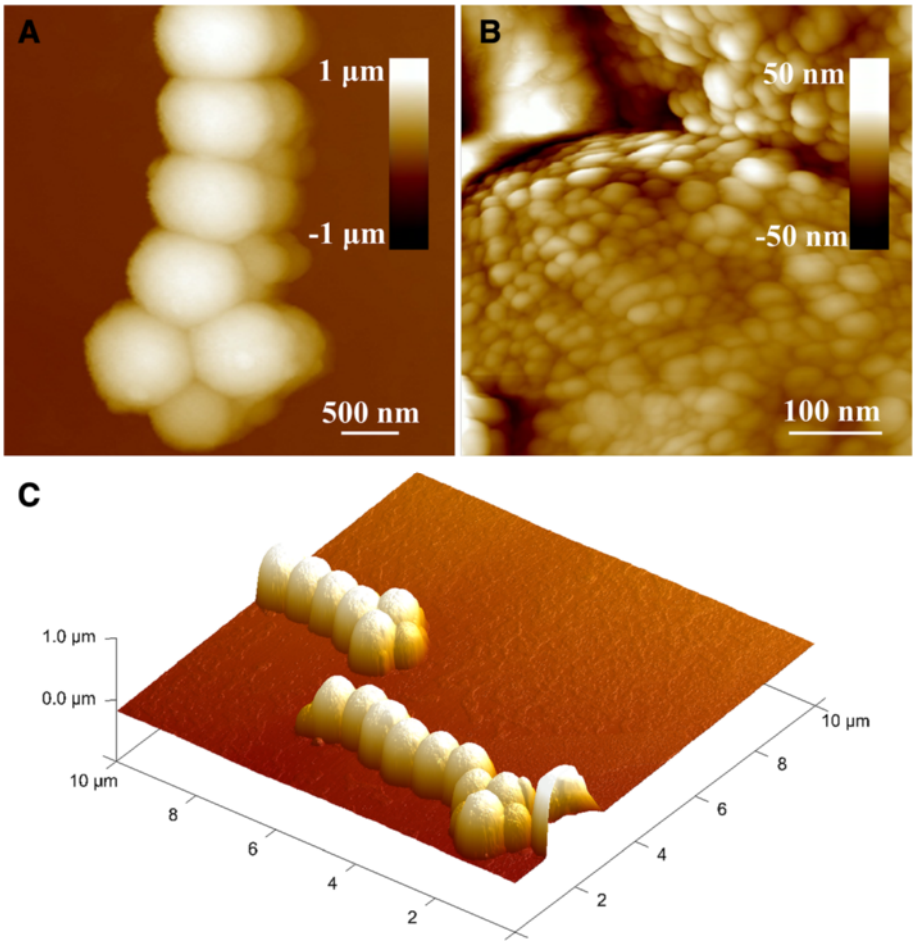

Figure 2 Surface morphology of the as-obtained Fe3O4 particles. (A) AFM image of Fe_3O_4 particles. **(B)** The enlarged AFM image of the isolated particles. **(C)** 3D image reconstruction of Fe_3O_4 particles.

ligand *in situ*, which was essential for their long-term stability in aqueous media without any surface modification.

Methods

Synthesis of Fe_3O_4 particles

In a typical synthesis of 725 nm Fe_3O_4 particles, 1.3 g of anhydrous $FeCl_3$ was first vigorously mixed with 40 mL of ethylene glycol (EG) to form a clear solution. Then, 0.47 g of EDTA was added and the mixture was heated at 110°C, followed by dissolving of anhydrous sodium acetate (NaOAc) (2.4 g), Then the mixture was transferred into a 100-mL Teflon-lined stainless-steel autoclave and sealed in air. The autoclave was kept at 200°C for 10 h. The black products were collected by a magnet and washed with ethanol three times, and the products were dried at 60°C for further use.

Characterizations

The x-ray diffraction (XRD) patterns were collected between 20° and 80° (2θ) on an x-ray diffraction system (X'Pert Pro, PANalytical Co., Almelo, The Netherlands) with a graphite monochromator and Cu Kα radiation (λ = 0.15406 nm). Transmission electron microscope (TEM) images and selected area electron diffraction (SAED) patterns were obtained (JEOL JEM-2100; JEOL, Tokyo, Japan) operated at an accelerating voltage of 200 kV. The samples for TEM and high-resolution transmission electron microscope (HR-TEM) analyses were prepared by spreading a drop of as-prepared magnetite nanoparticle-diluted dispersion on copper grids coated with a carbon film followed by evaporation under ambient conditions. Atom force microscope (AFM) characterization was carried out using Scan Asyst-Air (Bruker Multimode 8, Bruker Corporation, Billerica, MA, USA). Measurements were carried out in air, and imaging was performed in tapping mode. The height, amplitude, and phase images were recorded. The scanning electron microscopy (SEM) images were obtained using LEO 1530 microscope (LEO, Munich, Germany).

Results and discussion

The morphology of the as-prepared Fe_3O_4 particles was characterized by SEM (Figure 1). As shown in Figure 1A, when $FeCl_3$ concentration is low (0.05 mol L^{-1}), the products are nonuniform, consisting of spherical nanocrystal clusters and small nanocrystal aggregations. However, when the $FeCl_3$ concentration is in the range of 0.10 to 0.20 mol L^{-1}, all of Fe_3O_4 particles have a nearly spherical shape (Figure 1B,C). The diameters of the particles slightly increase from 622 ± 145 nm to 717 ± 43 nm, but their sizes become more uniform with the increase of $FeCl_3$ concentration, indicating that higher $FeCl_3$

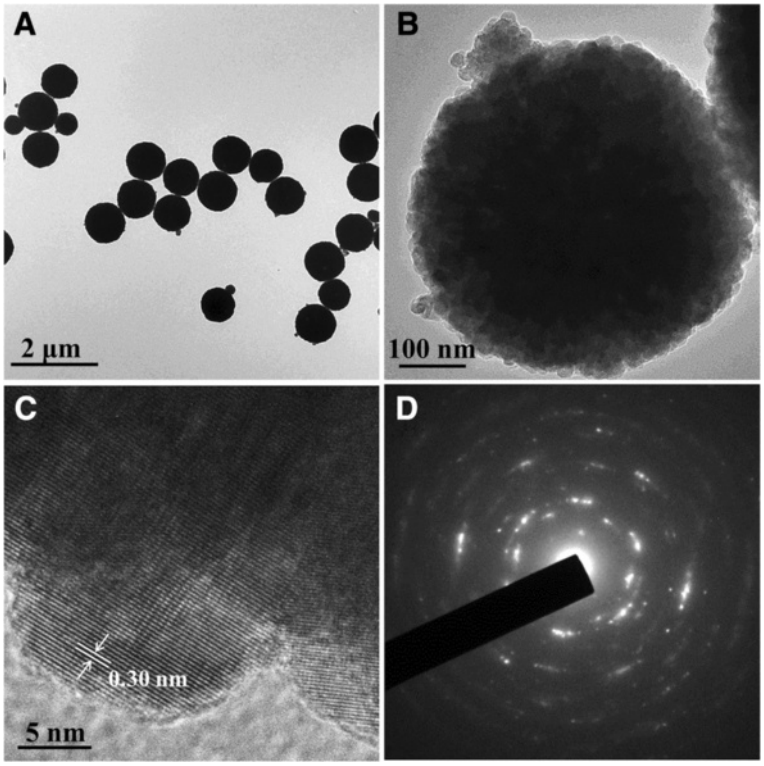

Figure 3 Uniform sizes and morphology of the as-prepared Fe_3O_4 particles. TEM images **(A, B)** and HR-TEM image **(C)** of the as-prepared Fe_3O_4 particles. SAED pattern of the particle in B **(D)**.

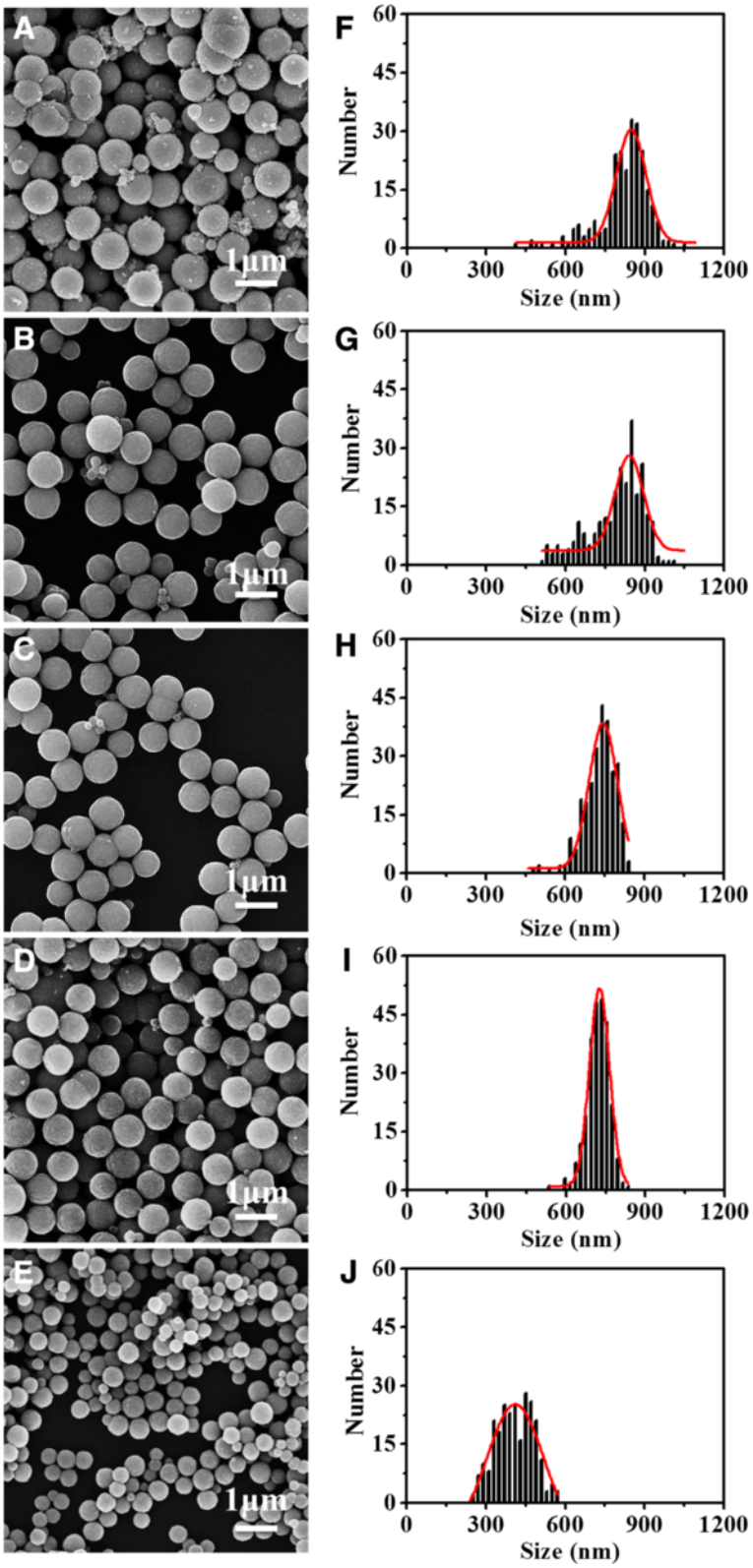

Figure 4 TEM images and XRD patterns of Fe_3O_4 particles. (A-E) TEM images and **(F-J)** XRD patterns of Fe_3O_4 particles synthesized with different EDTA concentrations: 0, 10, 20, 40, and 80 mol L^{-1}, respectively.

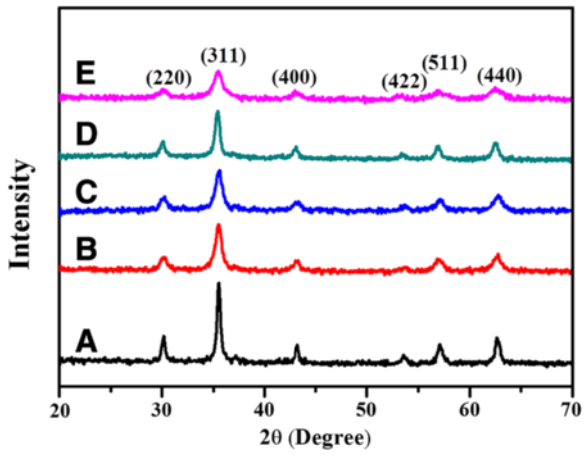

Figure 5 XRD patterns of Fe_3O_4 particles synthesized with different EDTA concentrations. (A) 0, (B) 10, (C) 20, (D) 40, and (E) 80 mol L^{-1}, respectively.

concentrations could lead to a larger and more uniform particle size.

The surface morphology of the as-obtained Fe_3O_4 particles is further shown in Figure 2. The 2D and 3D AFM images of Fe_3O_4 particles prepared from 0.20 mol L^{-1} of $FeCl_3$ appear a nearly uniform size of about 725 nm and spherical shape, which is in good agreement to the SEM results (Figure 1C). Furthermore, a high-resolution AFM image of an isolated Fe_3O_4 particle (Figure 2B) also indicates that the as-prepared Fe_3O_4 particles are composed of small nanocrystals with the size of about 7 to 15 nm.

TEM image of the as-prepared Fe_3O_4 particles (Figure 3A) further demonstrates their uniform sizes and morphology. The secondary structure of Fe_3O_4 particles also could be observed more clearly in Figure 3B for the isolated cluster, indicating that the obtained Fe_3O_4 particles are compact clusters. The HR-TEM image recorded at the edge of the Fe_3O_4 particles is shown in Figure 3C. Measuring the distance between two adjacent planes in a specific direction gives a value of 0.30 nm, corresponding to the lattice spacing of (220) planes of cubic magnetite [21,22]. The SAED pattern (Figure 3D) shows polycrystalline-like diffraction, suggesting that the as-prepared Fe_3O_4 particles consist of magnetite nanocrystals.

The effects of EDTA concentration on the particle sizes and grain sizes of Fe_3O_4 particles are further investigated. Without addition of EDTA, the resultant products have a heterogeneous size distribution and their shapes are nonuniform (Figure 4A,F). When the initial EDTA concentration is increased from 10 to 40 mmol L^{-1}, the sizes of Fe_3O_4 particles decrease slightly from 794 ± 103 nm to 717 ± 43 nm (Figure 4B,C,D and 4G,H,I) and their size distribution becomes more uniform. However, when the EDTA concentration further increases to 80 mmol L^{-1}, their sizes decrease significantly to 409 ± 70 nm while their size distribution becomes heterogeneous again (Figure 4E,J), indicating that higher EDTA concentration favors the formation of Fe_3O_4 particles with larger size; their size distribution, however, is EDTA concentration dependent.

To confirm the effects of EDTA concentration on the grain sizes and the corresponding crystalline structures and phase composition of the as-prepared Fe_3O_4 particles, the samples obtained with different EDTA concentrations are characterized by XRD. As shown in Figure 5, all the diffraction peaks are indexed to the spinel structure, known for the Fe_3O_4 crystal (JCPDS no. 00-003-0863) and no other peaks are detected, indicating that the products are pure phase Fe_3O_4. In addition, as the EDTA concentration increases, the broadening in the diffraction peaks becomes more pronounced. The grain sizes of the

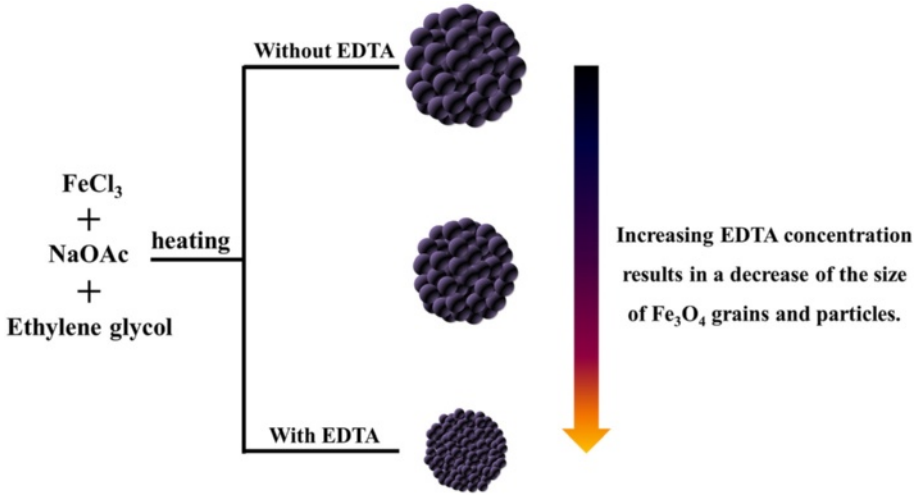

Figure 6 Schematic representation of the formation of Fe_3O_4 particles with tunable grain size and particle size.

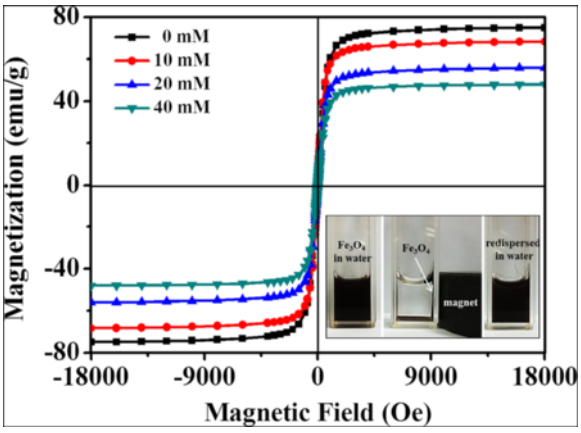

Figure 7 Hysteresis loops of the Fe_3O_4 particles obtained with EDTA concentrations. Inset was the photographs of an aqueous solution of Fe_3O_4 particles without magnetic field and with the externally applied magnetic field.

Fe_3O_4 particles calculated from the breadth of the (311) reflection using Debye-Scherrer's formula [23,24] decrease dramatically from 14.8 to 7.6 nm when the initial EDTA concentration increases from 0 to 80 mmol L^{-1}. It is thus concluded that EDTA could act as a stabilizer, which might significantly suppress the grain growth of the as-synthesized Fe_3O_4 particles.

As a consequence, a probable mechanism which leads to the resulting Fe_3O_4 particles with tunable grain size and particle size is proposed as follows (Figure 6). When EDTA is introduced to the $FeCl_3$/EG solution, a significant amount of Fe-EDTA complex is formed. NaOAc is then added and utilized as an alkali source. In the presence of EG and EDTA, Fe_3O_4 crystallites are formed first under alkaline condition, followed by further growth into Fe_3O_4 nanoparticles as the prolonging of reaction time in this system. The primary Fe_3O_4 nanoparticles then gradually aggregate into large particles to minimize the surface energy. In addition, because of the strong coordination between Fe(III) ions and carboxylate on the surface of particles [9,14,25], the as-prepared Fe_3O_4 particles also possess a coating of carboxylate and could be easily dispersed in water (inset in Figure 7). When a magnet is applied, the particles could be completely separated from the solution within seconds. Once the magnet is withdrawn, the particles could be redispersed into the water immediately by slight shaking. Furthermore, by increasing the amount of EDTA, more carboxylate groups could bind to the surface of Fe_3O_4 particles through the strong coordinating ligand. This results in a decrease of the size of Fe_3O_4 grains and particles. Magnetic properties (*M-H* curves) of Fe_3O_4 particles synthesized with EDTA over the concentration range of 0 to 40 mmol L^{-1} are shown in Figure 7. It is obvious that all the Fe_3O_4 particles have no remanence or coercivity at 300 K and their magnetic properties are strongly dependent on the sizes of Fe_3O_4 particles prepared. When the initial EDTA concentration is increased from 10 to 40 mmol L^{-1}, the sizes of Fe_3O_4 particles slightly decrease from 794 ± 103 nm to 717 ± 43 nm. Their magnetization saturation (Ms) values simultaneously suffer a corresponding decrease from 74.9 to 48.0 emu g^{-1}. This result also suggests that lower EDTA concentration favors the formation of Fe_3O_4 particles with better crystallinity, which is in good agreement to the XRD results.

Conclusions

In summary, a modified solvothermal approach was used to synthesize monodispersed Fe_3O_4 particles with the assistance of EDTA, which are composed of numerous primary Fe_3O_4 nanocrystals with sizes of 7 to 15 nm. Their sizes could be easily tuned over a wide range of 400 to 800 nm by simply varying the concentration of $FeCl_3$ or EDTA. More importantly, owing to the presence of the carboxylate groups attached on the surface, the Fe_3O_4 particles have excellent water dispersibility and dispersing stability. In addition, the growth mechanism of the secondary structural Fe_3O_4 particles is discussed. The magnetite particles are also superparamagnetic at room temperature and have a high magnetization, which enhance their response to external magnetic field and therefore should greatly facilitate the manipulation of the particles in practical uses.

Competing interests

The authors declare that they have no competing interests.

Authors' contributions

YY, YZ, and MJ performed the experiments. YW, LS, and YH were involved in experimental planning and analysis of the results. ZH and GZ designed and planned the experiment and LS also drafted the manuscript. All authors read and approved the final manuscript.

Acknowledgements

This work was supported by the Natural Science Foundation of China (grant nos. 31271071 and 81072472) and the Natural Science Foundation of Fujian Province (grant no. 2012 J01416) and The Medical Science and Technology Innovation Project of Nanjing Military Command (10MA078, 2010).

Author details

[1]The Affiliated Southeast Hospital of Xiamen University, Zhangzhou 363000, China. [2]Department of Radiology, Taishan Medical University, Taishan, Shandong 271016, China. [3]Research Center of Biomedical Engineering, Department of Biomaterials, College of Materials, Xiamen University, Xiamen 361005, China. [4]Organ Transplantation Institute, Medical College, Xiamen University, Xiamen 361005, China. [5]Anti-Cancer Research Center, Medical College, Xiamen University, Xiamen 361005, China.

Received: 18 December 2013 Accepted: 8 January 2014
Published: 14 January 2014

References

1. Majeed MI, Lu Q, Yan W, Li Z, Hussain I, Tahir MN, Tremel W, Tan B: **Highly water-soluble magnetic iron oxide (Fe_3O_4) nanoparticles for drug delivery: enhanced in vitro therapeutic efficacy of doxorubicin and MION conjugates.** *J Mater Chem B* 2013, **1**:2874–2884.

2. Veiseh O, Gunn J, Zhang M: **Design and fabrication of magnetic nanoparticles for targeted drug delivery and imaging.** *Adv Drug Deliv Rev* 2010, **62:**284–304.
3. Hao R, Xing R, Xu Z, Hou Y, Gao S, Sun S: **Synthesis, functionalization, and biomedical applications of multifunctional magnetic nanoparticles.** *Adv Mater* 2010, **22:**2729–2742.
4. Xu F, Geiger JH, Baker GL, Bruening ML: **Polymer brush-modified magnetic nanoparticles for his-tagged protein purification.** *Langmuir* 2011, **27:**3106–3112.
5. Xie J, Liu G, Eden HS, Ai H, Chen X: **Surface-engineered magnetic nanoparticle platforms for cancer imaging and therapy.** *Acc Chem Res* 2011, **44**(10):883–892.
6. Hayashi K, Ono K, Suzuki H, Sawada M, Moriya M, Sakamoto W, Yogo T: **One-pot biofunctionalization of magnetic nanoparticles via thiol – ene click reaction for magnetic hyperthermia and magnetic resonance imaging.** *Chem Mater* 2010, **22:**3768–3772.
7. Yoo D, Lee JH, Shin TH, Cheon J: **Theranostic magnetic nanoparticles.** *Acc Chem Res* 2011, **44**(10):863–874.
8. Li Z, Yi PW, Sun Q, Lei H, Li Zhao H, Zhu ZH, Smith SC, Lan MB, Lu GQ: **Ultrasmall water-soluble and biocompatible magnetic iron oxide nanoparticles as positive and negative dual contrast agents.** *Adv Funct Mater* 2012, **22:**2387–2393.
9. Shen L, Bao J, Wang D, Wang Y, Chen Z, Ren L, Zhou X, Ke XB, Chen M, Yang AQ: **One-step synthesis of monodisperse, water-soluble ultra-small Fe_3O_4 nanoparticles for potential bio-application.** *Nanoscale* 2012, **5:**2133–2141.
10. Hu F, MacRenaris KW, Waters EA, Liang T, Schultz-Sikma EA, Eckermann AL, Meade TJ: **Ultrasmall, water-soluble magnetite nanoparticles with high relaxivity for magnetic resonance imaging.** *J Phys Chem C* 2009, **113:**20855–20860.
11. Ngo TH, Tran DL, Do HM, Tran VH, Le VH, Nguyen XP: **Facile and solvent-free routes for the synthesis of size-controllable Fe3O4 nanoparticles.** *Adv Nat Sci* 2010, **1:**035001.
12. Wu S, Sun A, Zhai F, Wang J, Xu W, Zhang Q, Volinsky AA: **Fe_3O_4 magnetic nanoparticles synthesis from tailings by ultrasonic chemical co-precipitation.** *Mater Lett* 2011, **65:**1882–1884.
13. Liu Y, Liu P, Su Z, Li F, Wen F: **Attapulgite–Fe_3O_4 magnetic nanoparticles via co-precipitation technique.** *Appl Surf Sci* 2008, **255:**2020–2025.
14. Mejías R, Perez-Yague S, Gutiérrez L, Cabrera LI, Spada R, Acedo P, Serna CJ, Lázaro FJ, Villanueva A, Morales MP, Barber DF: **Dimercaptosuccinic acid-coated magnetite nanoparticles for magnetically guided in vivo delivery of interferon gamma for cancer immunotherapy.** *Biomaterials* 2011, **32:**2938–2952.
15. Wang X, Zhao Z, Qu J, Wang Z, Qiu J: **Shape-control and characterization of magnetite prepared via a one-step solvothermal route.** *Cryst Growth Des* 2010, **7**(10):2863–2869.
16. Lee SH, Yu S-H, Lee JE, Jin A, Lee DJ, Lee N, Jo H, Shin K, Ahn TY, Kim YW, Cheo H, Sung YE, Hyeon T: **Self-assembled Fe3O4 nanoparticle clusters as high-performance anodes for lithium ion batteries via geometric confinement.** *Nano Lett* 2013, **13:**4249–4256.
17. Gao J, Ran X, Shi C, Cheng H, Cheng T, Su Y: **One-step solvothermal synthesis of highly water-soluble, negatively charged superparamagnetic Fe_3O_4 colloidal nanocrystal clusters.** *Nanoscale* 2013, **5:**7026–7033.
18. Qiu P, Jensen C, Charity N, Towner R, Mao C: **Oil phase evaporation-induced self-assembly of hydrophobic nanoparticles into spherical clusters with controlled surface chemistry in an oil-in-water dispersion and comparison of behaviors of individual and clustered iron oxide nanoparticles.** *J Am Chem Soc* 2010, **132:**17724–17732.
19. Chang EP, Hatton TA: **Membrane emulsification and solvent pervaporation processes for the continuous synthesis of functional magnetic and Janus nanobeads.** *Langmuir* 2012, **28:**9748–9758.
20. Toprak MS, McKenna BJ, Mikhaylova M, Waite JH, Stucky GD: **Spontaneous assembly of magnetic microspheres.** *Adv Mater* 2007, **19:**1362–1368.
21. Xie G, Xi P, Liu H, Chen F, Huang L, Shi Y, Hou F, Zeng Z, Shao C, Wang J: **A facile chemical method to produce superparamagnetic graphene oxide-Fe_3O_4 hybrid composite and its application in the removal of dyes from aqueous solution.** *J Mater Chem* 2012, **22:**1033–1039.
22. Cheng W, Tang K, Qi Y, Sheng J, Liu Z: **One-step synthesis of superparamagnetic monodisperse porous Fe_3O_4 hollow and core-shell spheres.** *J Mater Chem* 2010, **20:**1799–1805.
23. Xiao L, Shen H, von Hagen R, Pan J, Belkoura L, Mathur S: **Microwave assisted fast and facile synthesis of SnO_2 quantum dots and their printing applications.** *Chem Comm* 2010, **46:**6509–6511.
24. Zhang S, Liu X, Zhou L, Peng W: **Magnetite nanostructures: one-pot synthesis, superparamagnetic property and application in magnetic resonance imaging.** *Mater Lett* 2012, **68:**243–246.
25. Charkoudian LK, Franz KJ: **Fe(III)-coordination properties of neuromelanin components: 5,6-dihydroxyindole and 5,6-dihydroxyindole-2-carboxylic acid.** *Inorg Chem* 2006, **45:**3657–3664.

doi:10.1186/1556-276X-9-27
Cite this article as: Yi *et al.*: Ethylenediaminetetraacetic acid as capping ligands for highly water-dispersible iron oxide particles. *Nanoscale Research Letters* 2014 **9**:27.